INTERNATIONAL JOURNAL FOR NUMERICAL METHODS IN FLUIDS
Int. J. Numer. Meth. Fluids 2004; **46**:1007–1024
Published online 27 September 2004 in Wiley InterScience (www.interscience.wiley.com). DOI: 10.1002/fld.784

A simple strategy for constructing bounded convection schemes for unstructured grids

Peter L. Woodfield[1,*,†], Kenjiro Suzuki[2,‡] and Kazuyoshi Nakabe[3,§]

[1]*Institute of Ocean Energy, Saga University, 1-Honjo-machi, Saga-shi, Saga 840-8502, Japan*
[2]*Department of Machinery and Control Systems, Shibaura Institute of Technology, Fukasaku 307, Minuma-ku, Saitama 337-8570, Japan*
[3]*Applied Energy Science Laboratory, Department of Energy System Engineering, Osaka Prefecture University, Sakai, Osaka 599-8531, Japan*

SUMMARY

Due to the great geometrical flexibility, popularity for unstructured grid methods in fluid dynamics has been increasing in recent years. In parallel with this interest there is a need for bounded second or higher order convection schemes which can be implemented easily in the unstructured setting. In the present work a simple strategy for achieving convective boundedness in the context of a vertex-centered unstructured finite volume algorithm is demonstrated. Testing is carried out on an inviscid oblique step problem using both structured and unstructured grid arrangements. Further testing for numerical diffusion is done using a distorted grid in a two dimensional channel. The proposed scheme is straightforward to implement and is found to perform well for the cases considered. The overall algorithm converges well and the limiter appears to introduce little extra numerical diffusion beyond that inherently present in the base scheme. Copyright © 2004 John Wiley & Sons, Ltd.

KEY WORDS: unstructured grid; boundedness; limiter; convection scheme

1. INTRODUCTION

In using second or higher-order convection schemes problems can often arise as a result of physically unrealistic overshoots or undershoots in the vicinity of sudden changes in the gradients of the dependent variables. These problems are particularly noticeable for parameters such as k and ε which cannot be less than zero and species concentrations which must fall

*Correspondence to: P. L. Woodfield, Institute of Ocean Energy, Saga University, 1-Honjo-machi, Saga-shi, Saga 840-8502, Japan.
†E-mail: peter@me.saga-u.ac.jp
‡E-mail: ksuzuki@sic.shibaura-it.ac.jp
§E-mail: nakabe@energy.osakafu-u.ac.jp

Contract/grant sponsor: Japan Science and Technology Corporation (JST)
Contract/grant sponsor: Japan Society for the Promotion of Science (JSPS)

Received 6 January 2003
Revised 22 January 2004

between zero and one. A commonly used solution is to employ higher order schemes for components of velocity only and first order upwind differencing schemes for the obviously problematic variables. This may have some justification in some cases, however as has been noted [1], first order schemes can introduce a significant amount of additional numerical diffusion. A better solution is to keep the higher order scheme for all variables and use a numerical device that in the literature is often called a 'limiter' to control the convection scheme in the vicinity of rapid gradient changes. While a number of effective limiters have been devised in the last twenty years (for example References [1–8] and the references contained therein), relatively few have been designed specifically with unstructured grids in mind (for example References [3–6]). It is possible to apply structured grid limiters to unstructured grids [9, 10] but it can be somewhat inconvenient particularly if the procedure requires interpolation of additional upstream points. In the present work we outline a general strategy for achieving bounded solutions by making use of principles similar to those suggested by Gaskell and Lau [2] and apply it to a second order upwind biased scheme in the setting of a vertex centred unstructured finite volume algorithm. The main contribution of the present work is in demonstrating that a very simple approach can be used to produce quite acceptable monotone solutions for incompressible flow calculation on unstructured grids.

2. OVER-VIEW OF DISCRETIZATION PROCEDURE FOR NAVIER–STOKES EQUATIONS

Before focusing on the limiter it is useful to make a brief overview of the underlying numerical scheme. Full details can be found in the previous work of the authors [11].

The mathematical equations for the dependent variables, u, v, w, h, etc. are all cast into the form of Equation (1).

$$\frac{\partial}{\partial x_j}(\rho u_j \phi) = \frac{\partial}{\partial x_j}\left(\Gamma \frac{\partial \phi}{\partial x_j}\right) + b_{(\phi)} \tag{1}$$

Equation (1) is re-expressed in integral form using the divergence theorem for an arbitrary control volume shape as in Equation (2).

$$\iint_{\text{Surf}} (\rho u_j \phi n_j)\, \mathrm{d}s = \iint_{\text{Surf}} \left(\Gamma \frac{\partial \phi}{\partial x_j} n_j\right) \mathrm{d}s + \iiint_{\text{Vol}} (b_{(\phi)})\, \mathrm{d}v \tag{2}$$

It should be noted that mathematically Equation (2) is an exact representation of Equation (1) regardless of the shape or orientation of the control volume with respect to a fixed Cartesian frame of reference. This fact is very convenient for the unstructured method since it makes it possible to use exactly the same Cartesian frame of reference for every control volume in the whole domain. Thus in the present approach we do not need to align the sides of the control volumes with the axis co-ordinates (as is shown below in Figure 1). Moreover it should be emphasized that also we do not need to transform Equation (2) to a generalized curvilinear co-ordinate system since the same Cartesian co-ordinate frame is used for the entire problem.

The computational grid may be constructed of tetrahedrons or hexahedrons in three dimensions and triangles or quadrilaterals in two dimensions. In the present approach, unknowns are solved at the corners of the polyhedrons (or polygons for two dimensions), which form the

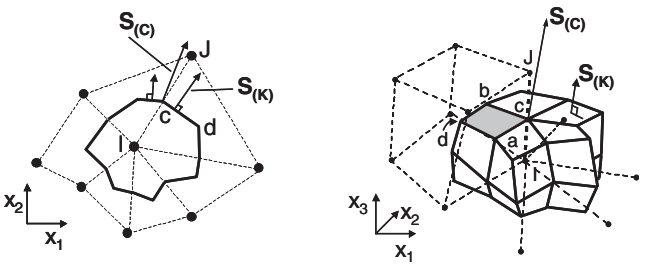

Figure 1. Control volumes used for numerical integration. (a) 2D mesh; (b) 3D mesh. '*c*' is the midpoint of the edge *I*–*J*, 'a' and 'b' are face centres of the hexahedron and 'd' is the centre of the hexahedron shown.

building blocks for the mesh. Median–dual control volumes as shown in Figure 1 are used for numerical discretization of Equation (2).

In Figure 1 the line connecting any two neighbouring points (e.g. *I*–*J*) is generally called an 'edge'. If in numerical integration, we can assume that the values of any variables interpolated to the edge midpoint '*c*' are representative of all the facets of the control volume which have a corner at '*c*' (see Figure 1(b)), then the geometry for the entire domain can be summarized as a set of vectors $\{S_{(c)}\}$ where there is one vector for each edge. For any given edge *I*–*J* in Figure 1(b), $S_{(c)}$ is simply the vector sum of the facet area vectors $S_{(k)}$ for facets with a corner at '*c*'. $S_{(k)}$ is normal to the facet and has a magnitude equal to the area of the facet. In the two-dimensional case (Figure 1(a)), $S_{(k)}$ has a magnitude equal to the length of the line *c*–*d* and unlike the three-dimensional case there are only two vectors which need to be added together to calculate $S_{(c)}$ for each edge.

Numerical integration over the control volume for each term in Equation (2) is carried out as explained in the sections below. The continuity and momentum equations are linked in an iterative procedure utilizing the SIMPLE algorithm [12]. Individual discretized equations are solved using under-relaxed Jacobi point iterations using the edge-based data structure as explained in the Appendix of this paper.

3. NUMERICAL TREATMENT OF THE CONVECTION SCHEME

3.1. Base convection scheme

The term on the left in Equation (2) is discretized as given in Equation (3) where the summation is done over all edges associated with the control volume surrounding the point '*I*'.

$$\iint_{\text{Surf}} \rho u_j \phi n_j \, \mathrm{d}s \approx \sum_{\text{NIneighbours}} \rho|_{\text{C}} \phi|_{\text{C}} \mathbf{u}|_{\text{C}} \bullet \mathbf{S}_{(\text{C})} \tag{3}$$

As can be seen in this equation the discretization method finally reduces to how we decide to interpolate the values of 'ρ', 'ϕ' and the dot product '$u_j S_j$' to the edge midpoint '*c*'.

The authors have selected linear interpolation for property variables, a second order upwind biased interpolation for the dependent variable, ϕ and the Rhie and Chow [13] approach for interpolating the volume flux term '$u_j S_j$'. This combination has been found to work quite well [11] and it allows us to use a co-located grid for pressure and velocity components without producing an erroneous 'checker board' effect in the pressure distribution.

In the present article, we will focus on the method for interpolating the dependent variable, ϕ to the midpoint 'c' in Equation (3) since this is where the limiter is applied to the scheme. For a given edge, if 'I' is the upwind point then $\phi|_c$ is given by Equation (4).

$$\phi|_C = \phi|_I + \Psi \frac{\Delta_{(IJ)}}{2} \times \frac{\partial \phi}{\partial X}|_I \tag{4}$$

In this equation, upper-case 'X' denotes the direction I–J and $\Delta_{(IJ)}$ the distance from 'I' to 'J'. The Greek letter Ψ represents the limiter and has values ranging from zero (fully limited scheme) to one (base scheme) as will be explained below. To calculate the gradient at the upstream point in Equation (4) we use another numerical approximation to the divergence theorem as given in Equation (5).

$$\frac{\partial \phi}{\partial x_i}|_I \approx \frac{1}{\mathrm{Vol}_{(I)}} \left(\sum_{\mathrm{NIneighbours}} \frac{1}{2}(\phi|_I + \phi|_J) S_i|_C \right) \tag{5}$$

The component of the gradient vector in Equation (5) along the direction I–J is given by Equation (6) where B_j is the 'j'th component of a unit vector along the direction I–J.

$$\frac{\partial \phi}{\partial X}|_I = \frac{\partial \phi}{\partial x_j}|_I B_j \tag{6}$$

It should be noted that in Equation (6) and throughout this paper Einstein's summation convention for Cartesian tensor notation is followed where the repeated subscript (in this case 'j') implies a summation from 1 to 3 for three dimensions or from 1 to 2 for two dimensions. Subscripts that follow a vertical bar or are in parenthesis (whichever is more convenient) are used to indicate labels that are not tensor subscripts.

If the value of Ψ used in Equation (4) is always set to unity then the scheme may allow non-physical over-shoots in the vicinity of rapid changes in gradient of the dependent variable. On the other hand if it is always set to zero then the entire domain will revert to a first order upwind scheme and much finer grid allocation will be required for an accurate solution. Thus the goal of the present approach is make good choices for the value of Ψ at different points in the computational domain so as to not permit overshoots and at the same time minimize numerical diffusion.

3.2. Strategy to produce bounded solutions

It should be noted that for many problems, higher order upwind biased convection schemes such as QUICK [14] (for structured grids) and the present unstructured second order scheme with Ψ set to unity can sometimes produce bounded solutions for the calculated distribution of the dependent variable, ϕ for most if not all of the domain in spite of the fact that the scheme itself is unbounded. In general it is found that overshoots and undershoots tend to occur in the vicinity of rapid changes in gradient of the variable ϕ and sometimes in places where the

gradient should be zero. This observation suggests that it would be strongly desirable if one could use the higher order scheme for as much of the domain as possible and then revert to a bounded first order upwind scheme only in regions where the higher order scheme produces values of ϕ which are unbounded by their neighbours. In fact, as will be shown below it is quite useful to think of the role of the limiter in terms of achieving this goal. For both structured and unstructured grids in multiple dimensions, a solution could be described as bounded if for every point 'I' in the domain Equation (7) is satisfied.

$$0 \leqslant \frac{\phi|_I - \phi_{(\text{min Ineighbour})}}{\phi_{(\text{max Ineighbour})} - \phi_{(\text{min Ineighbour})}} \leqslant 1 \tag{7}$$

In Equation (7) $\phi_{(\text{min Ineighbour})}$ is the minimum value of ϕ comparing all immediate neighbours of the point 'I' (not including $\phi|_I$ itself) and $\phi_{(\text{max Ineighbour})}$ is the maximum value of ϕ for the neighbours of point 'I' (again not including $\phi|_I$). In other words, if $\phi|_I$ does not go outside of the range of values for ϕ specified by its neighbours then the solution is bounded at the point 'I'.

Noting Equation (7), for convenience we introduce a dimensionless parameter γ as defined by Equation (8).

$$\gamma_{(I)} = \frac{\phi|_I - \phi_{(\text{min Ineighbour})}}{\phi_{(\text{max Ineighbour})} - \phi_{(\text{min Ineighbour})}} \tag{8}$$

The most important part of the present strategy is to revert to a bounded first order convection scheme if the conditions suggested by Equation (9) arise.

$$\gamma_{(I)} < 0 \text{ or } \gamma_{(I)} > 1 \Rightarrow \text{scheme} = \text{bounded 1st order} \tag{9}$$

Simply using the second order scheme everywhere else except at grid points where Equation (9) applies is found to fail since there is not a smooth shift between the second order and first order schemes. The limiter then switches on and off from iteration to iteration and convergence is never reached. So the strategy also needs to satisfy Equation (10).

$$\gamma_{(I)} \to 0 \text{ or } \gamma_{(I)} \to 1 \Rightarrow \text{scheme} \to \text{bounded 1st order} \tag{10}$$

Finally to make the strategy complete Equation (11) gives the range of γ for which the second order scheme should be employed.

$$\delta \leqslant \gamma_{(I)} \leqslant 1 - \delta \Rightarrow \text{scheme} = \text{unbounded 2nd order} \tag{11}$$

In Equation (11) the parameter δ needs to be chosen somewhere in the range from 0 to 0.5 and if γ approaches δ from below (i.e. if $0 < \gamma < \delta$ and $\gamma \to \delta$) or $1 - \delta$ from above (i.e. if $1 - \delta < \gamma < 1$ and $\gamma \to 1 - \delta$) then the scheme should approach the unbounded second order base scheme to achieve good convergence.

3.3. Bounded first order scheme for case where limiter is fully switched on

Having examined the overall strategy we need to consider the details of the first order scheme to be applied in the case where the limiter is fully switched on. If the conditions suggested by Equation (9) and in the limit of Equation (10) arise then it is essential that the chosen first order scheme must truly be bounded.

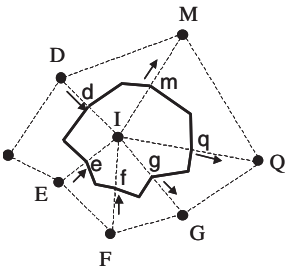

Figure 2. Example two-dimensional control volume for grid point '*I*'. Arrows indicate direction of flow for each edge in the example.

Without loss of generality, it is instructive to consider a two dimensional case such as that shown in Figure 2.

In this figure the points 'D', 'E' and 'F' are upstream of the point '*I*' while the points 'G', 'Q' and 'M' are downstream. The points given by lower case letters 'd', 'e', 'f', 'g', 'q', and 'm' are the midpoints of the edges '*I*–D', '*I*–E', '*I*–F', '*I*–G', '*I*–Q' and '*I*–M', respectively.

If in Equation (4) we set Ψ to zero for the grid point '*I*' then for the points 'g', 'q' and 'm' in Figure 2 the following relations apply:

$$\begin{aligned} \phi|_{\mathrm{g}} &= \phi|_I \\ \phi|_{\mathrm{q}} &= \phi|_I \\ \phi|_{\mathrm{m}} &= \phi|_I \end{aligned} \tag{12}$$

In a steady, pure convection problem the resulting equation for the variable $\phi|_I$ will be given by Equation (13):

$$F_{(\mathrm{d})}\phi|_{\mathrm{d}} + F_{(\mathrm{e})}\phi|_{\mathrm{e}} + F_{(\mathrm{f})}\phi|_{\mathrm{f}} = F_{(\mathrm{g})}\phi|_I + F_{(\mathrm{q})}\phi|_I + F_{(\mathrm{m})}\phi|_I \tag{13}$$

where for example $F_{(\mathrm{d})}$ is the magnitude of the mass flux for the edge midpoint 'd'.

Now in order to satisfy continuity Equation (14) applies.

$$F_{(\mathrm{d})} + F_{(\mathrm{e})} + F_{(\mathrm{f})} = F_{(\mathrm{g})} + F_{(\mathrm{q})} + F_{(\mathrm{m})} = F_{(\mathrm{tot})} \tag{14}$$

Hence Equation (13) can be rewritten in the form given by Equation (15).

$$\phi|_I = \frac{F_{(\mathrm{d})}}{F_{(\mathrm{tot})}}\,\phi|_{\mathrm{d}} + \frac{F_{(\mathrm{e})}}{F_{(\mathrm{tot})}}\,\phi|_{\mathrm{e}} + \frac{F_{(\mathrm{f})}}{F_{(\mathrm{tot})}}\,\phi|_{\mathrm{f}} \tag{15}$$

In other words $\phi|_I$ is a positively weighted average of $\phi|_{\mathrm{d}}$, $\phi|_{\mathrm{e}}$ and $\phi|_{\mathrm{f}}$ and therefore we can say that $\phi|_I$ will be bounded by $\phi|_{\mathrm{d}}$, $\phi|_{\mathrm{e}}$ and $\phi|_{\mathrm{f}}$. Thus the first order part of the present scheme will be bounded if the values interpolated to the midpoints of the inflowing edges ('d', 'e' and 'f' in Figure 2) are also bounded by the neighbouring points. There are a number of possible ways to ensure that this requirement is met. Perhaps the simplest is to set $\phi|_{\mathrm{d}}$, $\phi|_{\mathrm{e}}$ and $\phi|_{\mathrm{f}}$ equal to $\phi|_{\mathrm{D}}$, $\phi|_{\mathrm{E}}$ and $\phi|_{\mathrm{F}}$, respectively (pure first order upwinding). In other words set Ψ to zero in Equation (4) if either of the grid points '*I*' or '*J*' require a bounded first order scheme. However in the context of the present strategy, this choice

is found to be a somewhat diffusive if the overall scheme is to transfer smoothly from the second to the first order convection scheme. A better approach is to follow the reasoning of Gaskell and Lau [2] and always insist on interpolative boundedness for neighbouring points. By interpolative boundedness we mean for example $\phi|_{\mathrm{d}}$ must lie between $\phi|_{\mathrm{D}}$ and $\phi|_I$ as given by Equation (16).

$$0 \leqslant \frac{\phi|_{\mathrm{d}} - \phi|_{\mathrm{D}}}{\phi|_I - \phi|_{\mathrm{D}}} < 1 \tag{16}$$

It is found that the requirement given by Equation (16) does not appear to introduce noticeable extra numerical diffusion to the second order scheme and as such it can be introduced everywhere in the domain and not just in regions where the first order scheme is active. Provided the extreme case where $\phi|_{\mathrm{d}} = \phi|_{\mathrm{e}} = \phi|_{\mathrm{f}} = \phi|_I$ does not occur then if Equation (16) is enforced, an unbounded value of $\phi|_I$ will iteratively progress towards being bounded by the values at the upstream points when the limiter is fully switched on (Ψ set to zero).

A third alternative which deserves mentioning since it is used in the unstructured grid convection scheme of Barth and Jesperson [3], requires that interpolated values to edge midpoints are always bounded by the maximum and minimum of all of the neighbours of the upstream grid point including the point itself. In terms of the interpolated point 'd' in Figure 2 this requirement is given by Equation (17).

$$0 \leqslant \frac{\phi|_{\mathrm{d}} - \mathrm{MIN}(\phi_{(\text{min Dneighbour})}, \phi|_{\mathrm{D}})}{\mathrm{MAX}(\phi_{(\text{max Dneighbour})}, \phi|_{\mathrm{D}}) - \mathrm{MIN}(\phi_{(\text{min Dneighbour})}, \phi|_{\mathrm{D}})} \leqslant 1 \tag{17}$$

Equation (17) is less restrictive than Equation (16) and at extremities where the limiter is fully switched on it produces a first order scheme that is bounded by the maximum and minimum of a group of surrounding points consisting of the upstream neighbouring points and their neighbours. The definition of boundedness in this case would be slightly relaxed from that given by Equation (7) but probably adequate for achieving physically realistic results since the gradient used in the interpolation of $\phi|_{\mathrm{d}}$ for example also makes use of these additional upstream neighbouring points (cf. Equation (5)). Nevertheless, for the present work we have selected the slightly more restrictive approach given by Equation (7) and have insisted on the requirements of Equation (16) everywhere in the domain.

3.4. Combined scheme with proposed limiter

Returning to the general edge '*I*–*J*' shown in Figure 1, the limiter is applied to the scheme for the case where '*I*' is upstream of '*J*' as follows. Firstly in Equation (4), Ψ is rewritten as given in Equation (18) where $\Psi_{(I)}$ is responsible for switching on the first order scheme when required and $\Psi_{(IJ)}$ is responsible for ensuring interpolative boundedness for the edge.

$$\Psi = \Psi_{(I)}\Psi_{(IJ)} \tag{18}$$

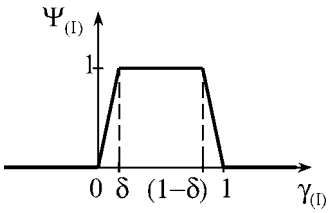

Figure 3. Present limiter (Equation (19)) plotted against the dimensionless parameter, γ (Equation (8)).

Equation (19) defines $\Psi_{(I)}$ in terms of the requirements given by Equations (9)–(11).

$$\begin{aligned}
&\Psi_{(I)} = 0 \quad \text{if } \gamma_{(I)} \geqslant 1 \text{ or } \gamma_{(I)} \leqslant 0 \\
&\Psi_{(I)} = 1 \quad \text{if } \delta \leqslant \gamma_{(I)} \leqslant 1 - \delta \\
&\Psi_{(I)} = \frac{\gamma_{(I)}}{\delta} \quad \text{if } 0 < \gamma_{(I)} < \delta \\
&\Psi_{(I)} = \frac{1 - \gamma_{(I)}}{\delta} \quad \text{if } 1 - \delta < \gamma_{(I)} < 1 \\
&\Psi_{(I)} = 1 \quad \text{if } \phi_{(\text{max Ineighbour})} - \phi_{(\text{min Ineighbour})} \leqslant 10^{-20}
\end{aligned} \tag{19}$$

The last requirement in Equation (19) avoids division by zero for defining $\gamma_{(I)}$ in Equation (8). For the present work a value of 0.2 is selected for δ and the sensitivity to this choice is discussed below. Equation (19) is illustrated graphically in Figure 3 where it is clear that the limiter is a piecewise continuous function of γ which satisfies the requirements of Equations (9)–(11).

To ensure interpolative boundedness (cf. Equation (16)), $\Psi_{(IJ)}$ is defined as follows:

$$\begin{aligned}
\Theta &= \text{MIN}\left(1, \frac{2(\phi|_J - \phi|_I)}{\Psi_{(I)} \partial\phi/\partial X|_I \Delta_{(IJ)}}\right) \\
\Psi_{(IJ)} &= \text{MAX}(0, \Theta)
\end{aligned} \tag{20}$$

3.5. Practical implementation of the scheme

Ideally, implicit procedures should be used where possible. However it is found much more convenient to explicitly evaluate Equation (5) and the second term on the right of Equation (4). Equations (18)–(20) are also evaluated explicitly. For the present work, the upwind part in Equation (4) is the only term in the convection scheme treated implicitly (first term on right hand side of Equation (4)). This kind of procedure (sometimes called a 'deferred correction approach') is straightforward to implement but it may allow overshoots and undershoots to occur prior to reaching the fully converged state. However once full convergence is achieved there should be no overshoots or undershoots greater than the computer rounding error.

On another related practical point, prior to convergence, the continuity equation (cf. Equation (14)) may not be satisfied exactly so it is better to subtract the continuity equation multiplied by $\phi|_I$ from Equation (3) so that positively weighted averaging can always apply

to the implicit part of the scheme (cf. Equation (15)). Thus Equation (3) is rewritten as given in Equation (21) for the steady-state case.

$$\iint_{\text{Surf}} \rho u_j \phi n_j \, \mathrm{d}s \approx \sum_{\text{NIneighbours}} \rho|_{\text{C}}(\phi|_{\text{C}} - \phi|_I)\mathbf{u}|_{\text{C}} \bullet \mathbf{S}_{(\text{C})} \tag{21}$$

Also, it should be noted here that the deferred correction procedure does not in and of itself produce a bounded scheme due to the presence of the non-zero explicit source term.

4. NUMERICAL TREATMENT OF THE DIFFUSION TERMS

Although we have not mentioned the presence of the diffusion terms from the Navier–Stokes equations in any of the above discussion in reality the diffusion terms tend to reduce the need for a limiter. In terms of the dimensionless parameter $\gamma_{(I)}$ given by Equation (8), adding molecular diffusion will generally push $\gamma_{(I)}$ towards the centre of the bounded region given by Equation (7) and hence the diffusion terms will tend to switch off the limiter if it is not needed. Thus the present approach of aiming to only use the first order convection scheme when it is really necessary is well suited to convection/diffusion problems. The discretization for the diffusion terms is given in Equation (22) and the approximation for the gradient at the midpoint 'c' is given in Equation (23).

$$\iint_{\text{Surf}} \left(\Gamma \frac{\partial \phi}{\partial x_j} n_j \right) \mathrm{d}s \approx \sum_{\text{NIneighbours}} \Gamma|_{\text{C}} \frac{\partial \phi}{\partial x_j}|_{\text{C}} S_j|_{\text{C}} \tag{22}$$

$$\frac{\partial \phi}{\partial x_i}|_{\text{C}} \approx \frac{\phi|_J - \phi|_I}{\Delta_{(IJ)}} B_i + \frac{1}{2}\left(\frac{\partial \phi}{\partial x_i}|_I + \frac{\partial \phi}{\partial x_i}|_J \right) - \frac{1}{2}\left(\frac{\partial \phi}{\partial x_j}|_I + \frac{\partial \phi}{\partial x_j}|_J \right) B_j B_i \tag{23}$$

The gradients on the right hand side of Equation (23) are calculated in the same manner as Equation (5) and again it should be noted that lower case 'i' and 'j' are tensor subscripts so the repeated 'j' is summed from 1 to 3 for three dimensions.

5. TESTING OF THE SCHEME

5.1. Oblique flow test

The first test chosen for the scheme is the standard oblique inviscid flow test [1, 2, 8]. The computational domain and boundary conditions are defined in Figure 4. For the present study we consider the case where θ is 35°. Figure 5 shows the computational grids considered.

Figure 5(a) shows a standard mesh with 23×23 grid points in each direction. Figure 5(b) shows an unstructured mesh constructed from triangles (796 points), which has been distorted deliberately in order to provide a good test for the unstructured scheme. Both grids are stored in the same unstructured format.

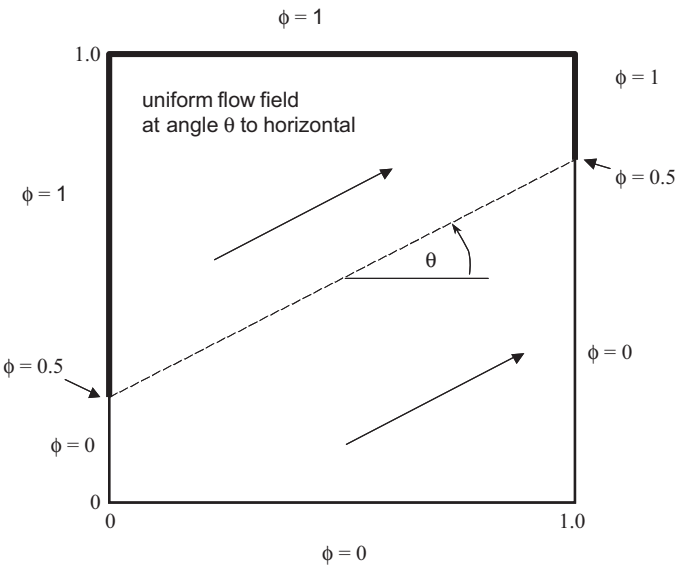

Figure 4. Domain and boundary conditions for the inviscid oblique flow problem.

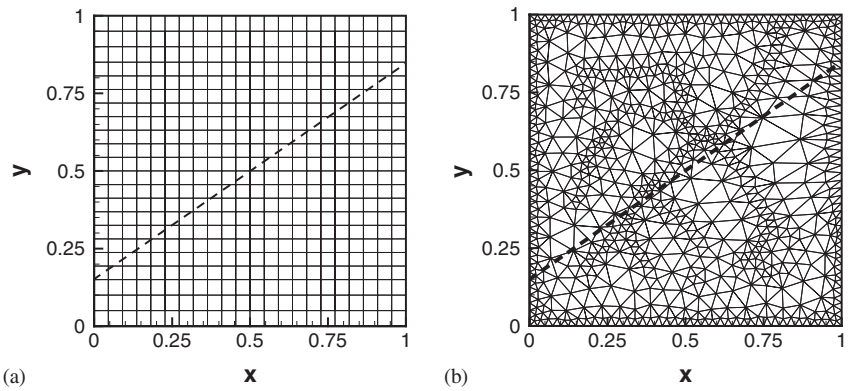

Figure 5. Computational grids used for oblique flow test. The dotted line shows the location of the step for the exact solution. (a) Quadrilateral mesh; (b) triangular mesh.

Figure 6 shows the performance of the present convection scheme with and without the limiter. Because the molecular viscosity is set to zero any departure from the step profile labeled 'exact' is due to the numerical discretization and the convection scheme. Predicted values of ϕ less than zero or greater than unity represent undershoots and overshoots, respectively. For reference purposes the grid spacing near the $x = 0.5$ centreline also is shown in Figure 6. As can be seen in Figure 6 the present limiter does not allow overshoots for both the quadrilateral and triangle mesh cases. Also the proposed approach is much less diffusive than

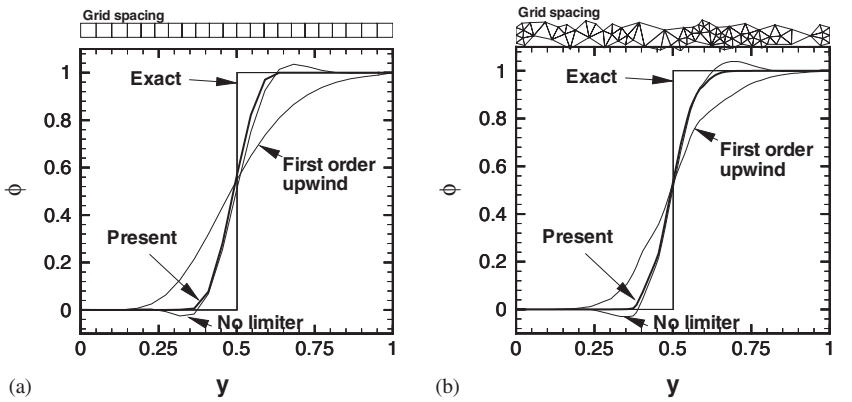

Figure 6. Present convection scheme with and without the limiter ($x = 0.5$). (a) Quadrilateral mesh; (b) triangular mesh.

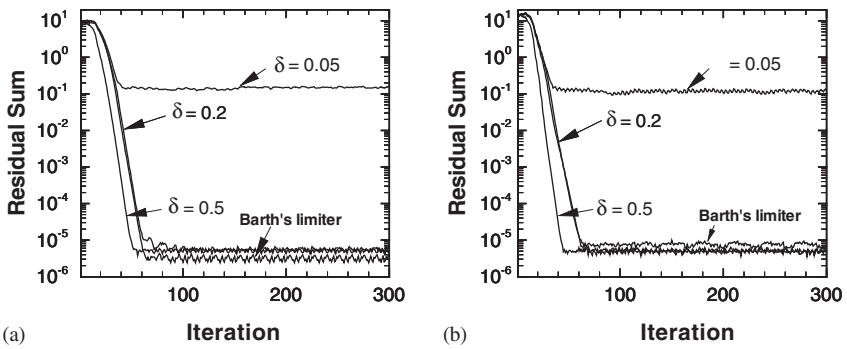

Figure 7. The effect of the choice of δ on convergence (the vertical axis shows the sum of the absolute value of the ϕ residual for the entire domain). (a) Quadrilateral mesh; (b) triangular mesh.

a first order upwind scheme. Not only for the profiles shown but for the entire domain the maximum overshoot was zero (i.e. less than $1.0\text{E}-8$ and thus not detectable with the present single precision calculation) and the maximum undershoot was of the order $-1.0\text{E}-12$ in both the triangle and quadrilateral mesh cases.

5.2. The choice of a value for the limiter switching constant

Concerning the choice of δ in Equation (19) two factors should be considered. The first relates to convergence. If the value of δ is too small the final level of convergence is much poorer. This is illustrated in Figure 7 which shows the sum of the residuals (see appendix) against the number of iterations for both the quadrilateral case Figure 6(a) and the triangle mesh case Figure 6(b). For the cases considered it appears that a value of 0.05 is too small while a value of 0.2 produces very good convergence. We might expect this since the limiter will tend to switch on and off more abruptly as δ approaches zero.

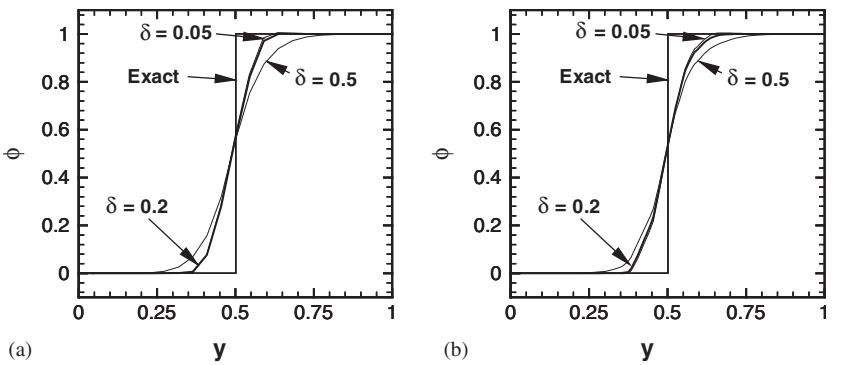

Figure 8. The effect of the choice of δ on numerical diffusion ($x = 0.5$). (a) Quadrilateral mesh; (b) triangular mesh.

The other factor that needs consideration in the choice of δ is its effect on numerical diffusion. We may expect that a smaller value of δ will be less diffusive than a larger value. This is quite reasonable since a larger δ implies that the range of values of γ for which the second-order scheme only is used (i.e. $\Psi = 1$) has diminished (cf. Figure 3). Figure 8 shows the effect of the choice of δ on the oblique flow case. The scheme becomes more diffusive as δ is increased to 0.5.

The curves for $\delta = 0.2$ and 0.05 are very similar in both cases shown in Figure 8. However, elsewhere in the domain setting $\delta = 0.05$ allowed an overshoot of around 2.0 per cent due to the poorer convergence and the explicit treatment. Thus a value of 0.2 is recommended for the present base scheme.

5.3. Comparison with Barth and Jesperson's limiter

It is useful to compare the present limiter with that of Barth and Jesperson [3] since their limiter has been reported to work well for flow calculation using unstructured grids [3]. Figure 9 compares results for the oblique test case using the present limiter and that of Barth and Jesperson applied to the present base scheme.

Quite clearly the performance of both limiters when applied to this problem is very good and quite similar. The final level of convergence achieved and rate of convergence for all four cases shown in Figure 9 was also quite similar. This can be seen in Figure 7(a) and 7(b) comparing the lines for $\delta = 0.2$ with the curves for Barth's limiter. The grid convergence rate is also found very similar to that resulting from the use Barth and Jesperson's limiter. An example is shown in Figure 10 using progressively finer grid spacing on the oblique step problem. These results indicate that the present approach is a comparable alternative for producing bounded results at least for incompressible flow situations.

The wiggles in the contours apparent in Figure 9(b) and 9(d) may be ascribed to the irregular triangular mesh shown in Figure 5(b).

In comparison to the approach of extending one dimensional limiters to unstructured grids by interpolating extra points on the upstream side of each edge, both the present limiter and Barth and Jesperson's scheme are significantly easier to implement in a general unstructured situation. This is because no special reference needs to be made to the shape of the

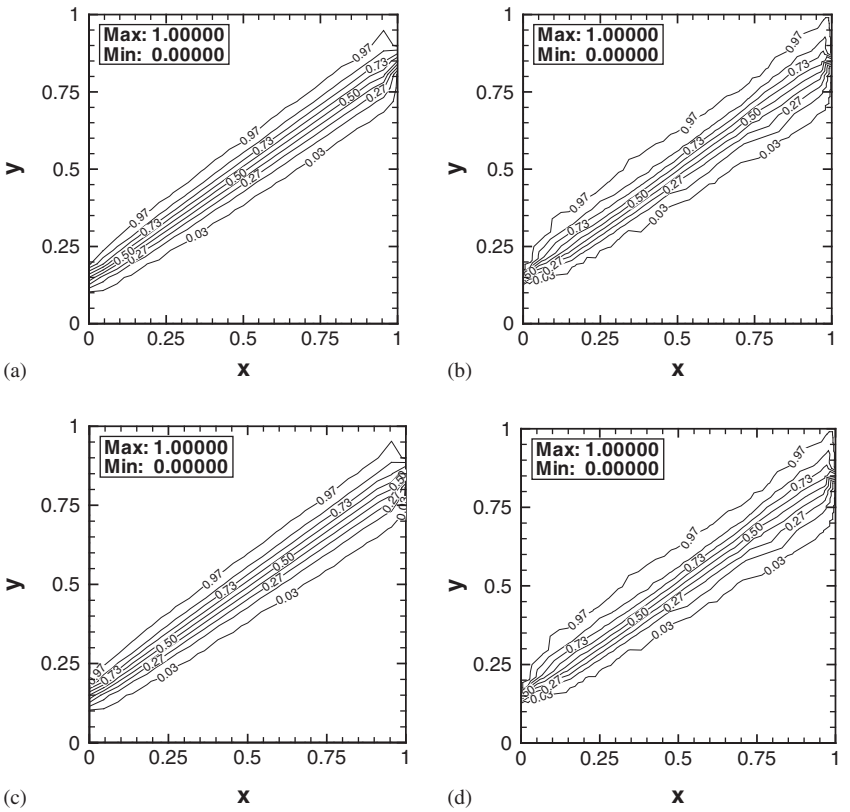

Figure 9. Comparison of results using present scheme with results using Barth and Jesperson's limiter [3] (ϕ distribution). (a) Quadrilateral—Present limiter; (b) Triangle—Present limiter; (c) Quadrilateral—Barth and Jesperson's limiter (d) Triangle—Barth and Jesperson's limiter.

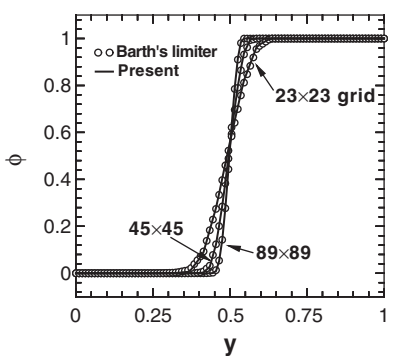

Figure 10. Grid convergence.

original building blocks for the computational mesh. Moreover, as has been demonstrated in Figure 9(b) and 9(d) that quite irregular meshes still yield monotone results using these limiters.

Computationally, the present approach requires one less loop over the edges than what is necessary for Barth and Jesperson's limiter and thus it is slightly less expensive to evaluate.

5.4. Application of the limiter to a central differencing convection scheme

A more rigorous test for the limiter is to apply it to a central differencing base convection scheme. In such a case Equation (24) is used instead of Equation (4) to obtain ϕ at the edge midpoint.

$$\phi|_C = \phi|_I + \Psi\tfrac{1}{2}(\phi|_J - \phi|_I) \tag{24}$$

Figure 11 shows the results of this test when applied to the oblique step problem in Figure 4. As can be seen in Figure 11(a) and 11(d), without the limiter, the central differencing scheme fails to give physically realistic results. The new limiter however yields quite acceptable monotone results for the whole domain for both triangle and quadrilateral meshes as can be seen in Figures 11(b) and 11(e). Also the limited central difference scheme is significantly less diffusive than the pure first order upwinding as can be seen by comparing Figures 11(b) and 11(e) with Figures 11(c) and 11(f). It should be noted that to obtain good convergence with the limiter applied to the central difference scheme, it was found necessary to raise the value of δ to 0.3. Comparing Figure 11(b) with Figure 9(a) it appears that the limiter applied to the central differencing scheme is slightly more diffusive than the scheme given by

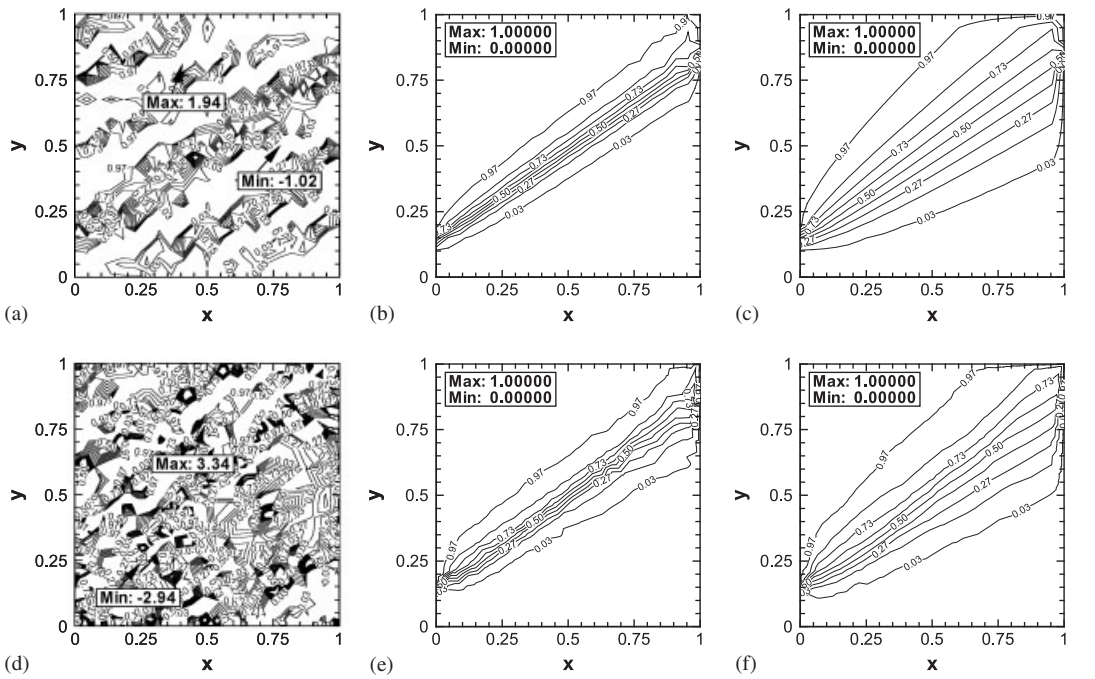

Figure 11. Effect of limiter applied to central differencing scheme. (ϕ distribution). Quadrilateral: (a) No limiter; (b) Present limiter $\delta = 0.3$; (c) First order upwind. Triangle: (d) No limiter; (e) Present limiter $\delta = 0.3$; (f) First order upwind.

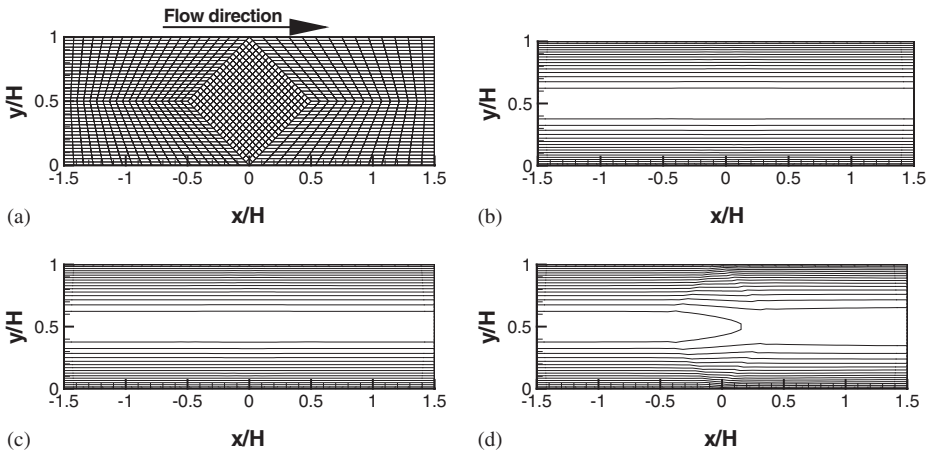

Figure 12. Fully developed 2D duct flow test case (u velocity contours). (a) Computational grid; (b) With limiter; (c) No limiter; (d) First order upwind.

Equation (4). This may be attributable to the higher value for δ. It also should be noted that for the triangle mesh case with central differencing as the base scheme, the present limiter converged significantly better than Barth and Jesperson's limiter applied to central differencing in the same case.

5.5. *Fully developed flow in 2D channel*

A further simple test for numerical diffusion is fully developed flow in a two dimensional channel having a mesh not aligned with the flow direction. Figure 12(a) shows the computational mesh for this test. A fully developed profile is specified at $x/H = -1.5$ and zero normal gradients are used for velocity components at $x/H = 1.5$. Reynolds number is set at 400 based on the channel height H and mean velocity.

By examining the results calculated without the limiter shown in Figure 12(c) it is clear that the limiter is not required for the present test case. Nevertheless, comparison of Figure 12(b) with 12(c) demonstrates that the present limiter does not introduce noticeably extra numerical diffusion when applied in situations where it is not essential. This is in contrast to first order upwinding (Figure 12(d)) which, while it guarantees a bounded solution, has the downside of severe numerical diffusion when the grid lines are not well aligned with the flow direction.

It should also be noted here that the Peclet number for the control volumes in the centre of the grid ($x/H = 0,\ \ y/H = 0$) in Figure 12 is approximately 15. Thus Figure 12 further demonstrates that the present approach has an advantage over advection schemes which use the Peclet number as the criterion for introducing first order upwinding.

6. CONCLUSIONS

A simple and effective strategy has been presented to produce bounded solutions on unstructured grids and yet allow the use of a second order convection scheme for the majority of the

calculation domain. The proposed limiter was applied to a second order upwind-biased base scheme in the context of a vertex-centred unstructured flow solver and found to perform well for grids based on triangles and quadrilaterals.

The procedure itself contains an adjustable parameter, δ, introduced in Equation (11) to control how gently the limiter switches on or off. A value of 0.05 for δ was found to result in poor convergence and overshoots for the oblique step flow problem. On the other hand setting δ to 0.5 produced a significant amount of numerical diffusion. It appears that a value of around 0.2 for the limiter switching constant δ is a good choice in terms of both reducing the size of the residuals whilst maintaining good resolution for the overall scheme.

For the incompressible flow situations considered, the performance and results were similar to those obtained using Barth and Jesperson's limiter [3]. Like Barth's limiter the present approach is completely general and is much easier to implement for three-dimensional unstructured grids than techniques which require the interpolation of additional nodes upstream of each edge to evaluate the limiter. The main advantage of the present approach over the alternatives for unstructured grids lies in its simplicity, both conceptually and in ease of implementation for any base convection scheme.

Finally, for all the cases considered the combination of the second-order scheme with the limiter appears to be a much better option than simply employing first order upwind biased schemes to preserve monotonicity.

NOMENCLATURE

$b_{(\phi)}$	source term
B_i	'i'th component unit vector in directions I–J in Figure 1
c	midpoint of line I–J
F	absolute value of mass flux
H	channel height
S_i	'i'th component of the vector $S_{(\mathrm{C})}$
$S_{(\mathrm{C})}$	vector representing the combined geometry of all facets of the control volume connected to point 'c'
$S_{(\mathrm{K})}$	vector representing the area and orientation of a single facet on the control volume surface
x_i	Cartesian co-ordinate
X	locally rotated Cartesian co-ordinate aligned with edge direction
x	Cartesian co-ordinate $(=x_1)$
y	Cartesian co-ordinate $(=x_2)$
ϕ	dependent variable
Γ	diffusion coefficient
ρ	density
$\Delta_{(IJ)}$	distance from point 'I' to point 'J'

APPENDIX A: UNSTRUCTURED GRID MATRIX SOLVER

It is useful to briefly describe the point Jacobi solver used in the present context as it illustrates the nature and convenience of the edge-based data structure for unstructured grids. It also

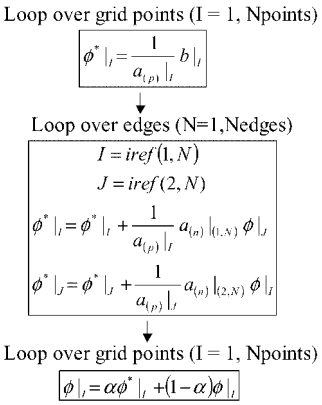

Figure A1. Algorithm for matrix solver using edge-based data structure.

illustrates how the coefficients for the discretized equations are stored in the computer program, which is useful information for unstructured code development and ultimately for application of the present limiter.

Equation (A1) is the discretized equation for the grid point 'I'.

$$a_{(\mathrm{p})}|_I \phi|_I = \sum_{\mathrm{NIneighbours}} (a_{(\mathrm{n})}|_{\mathrm{n}} \phi|_{\mathrm{n}}) + b|_I \tag{A1}$$

The dependent variable, ϕ, the diagonal coefficient, $a_{(\mathrm{p})}$, and the source term, b, are stored in one dimensional arrays having lengths equal to the total number of grid points. The coefficients for the neighbouring points, $a_{(\mathrm{n})}$ are stored on the edge-based structure where there are two coefficients for each edge in the domain. This approach is efficient as there is no limit to the number of neighbours a point can have and there is no need to store any zero coefficients for the sparse matrix.

The discretized equations are solved iteratively using an under-relaxed Jacobi point solver as shown in Figure A1. The first and third loops in this figure are over all grid points in the domain and the second loop is over all edges in the domain. In the present study the procedure given by Figure A1 is repeated four times prior to updating the coefficients, $a_{(\mathrm{p})}$, $a_{(\mathrm{n})}$ and b (i.e. four times per iteration). The under-relaxation factor, α is set to 0.6 for ϕ in the oblique step case, 0.5 for velocity and 0.6 for the pressure correction equation.

To vectorize the procedure shown in Figure A1 the only modification required is that the loop over the edges be divided up into a nested loop over groups of edges which do not have ends at common grid points. This stops the parallel machine trying to write to the same point at the same time.

Equation (A2) is used in calculating the residual sum for Figure 7.

$$R\mathrm{sum} = \sum_{I=1}^{\mathrm{Npoints}} |\phi|_I - \phi^*|_I| \tag{A2}$$

In this equation $\phi|_I$ has not yet been updated by the third loop shown in Figure A1.

ACKNOWLEDGEMENTS

This work was supported through the project 'Micro Gas Turbine/Fuel Cell Hybrid-Type Distributed Energy System' by the Japan Science and Technology Corporation (JST) as Core Research of Evolutional Science and Technology (CREST). The support of the Japan Society for the Promotion of Science (JSPS) for the first author also is gratefully acknowledged.

REFERENCES

1. Leonard BP, Drummond JE. Why you should not use 'hybrid', 'power-law' or related exponential schemes for convective modeling—there are much better alternatives. *International Journal for Numerical Methods in Fluids* 1995; **20**:421–442.
2. Gaskell PH, Lau AKC. Curvature-compensated convective transport: SMART, a new boundedness-preserving transport algorithm. *International Journal for Numerical Methods in Fluids* 1988; **8**:617–641.
3. Barth TJ, Jespersen DC. The design and application of upwind schemes on unstructured meshes. *AIAA paper* 89-0366, 1989.
4. Venkatakrishnan V. Convergence to steady state solutions of the Euler equations on unstructured grids with limiters. *Journal of Computational Physics* 1995; **118**:120–130.
5. Hubbard ME. Multidimensional slope limiters for MUSCL-type finite volume schemes on unstructured grids. *Journal of Computational Physics* 1999; **155**:54–74.
6. Jawahar P, Kamath H. A high-resolution procedure for Euler and Navier–Stokes computations on unstructured grids. *Journal of Computational Physics* 2000; **164**:165–204.
7. Van Albada GD, van Leer B, Roberts Jr WW. A comparative study of computational methods in cosmic gas dynamics. *Astronomy and Astrophysics* 1982; **108**:76–84.
8. Yu B, Tao WQ, Zhang DS, Wang QW. Discussion on numerical stability and boundedness of convective discretized schemes. *Numerical Heat Transfer Part B* 2001; **40**:343–365.
9. Cabello J, Morgan K. A comparison of higher order schemes used in a finite volume solver for unstructured grids. *AIAA Paper* 94-2293, 1994.
10. Jessee JP, Fiveland WA. A cell vertex algorithm for the incompressible Navier–Stokes equations on non-orthogonal grids. *International Journal for Numerical Methods in Fluids* 1996; **23**:271–293.
11. Woodfield PL, Nakabe K, Suzuki K. Performance of a three-dimensional pressure-based unstructured finite-volume method for low Reynolds number flow and wall heat transfer rate prediction. *Numerical Heat Transfer, Part B* 2003; **43**:403–423.
12. Patankar SV. *Numerical Heat Transfer and Fluid Flow*. Hemisphere Publishing Corporation: Washington, DC, 1980.
13. Rhie CM, Chow WL. Numerical study of the turbulent flow past an airfoil with trailing edge separation. *AIAA Journal* 1983; **21**:1525–1532.
14. Leonard BP. A stable and accurate convective modelling procedure based on quadratic upstream interpolation. *Computer Methods in Applied Mechanics and Engineering* 1979; **19**:59–98.

